



Research Article

Heat transfer enhancement by laterally impinging air jet on semi-circular grooved surface

A. M. RATHOD^{1,*}, Chandrashekhar K. JADHAV¹, Rohit S. TARTE¹, Nitin P. GULHANE¹,
Jan TALER², Dawid TALER², Pawel OCLON²

¹Department of Mechanical Engineering, VJTI, Mumbai, 400019, India

²Department of Energy, Cracow University of Technology, 31-864 Cracow, Poland

ARTICLE INFO

Article history

Received: 22 April 2024

Revised: 06 August 2024

Accepted: 11 August 2024

Keywords:

Cooling Rate; Jet Impingement; Local Nusselt Number; Reynold Number; Semicircular Groove Surface

ABSTRACT

This study experimentally investigates the cooling rate of a jet impinging on a semi-circular grooved surface. The experiments aim to determine the magnitude of convective heat dissipation on this grooved surface, which is 6mm thick and features six evenly distributed circular grooves. The investigation considers various factors, including Reynolds numbers ranging from 4000 to 12000, clearance (z/d) between nozzle outlet to target plate, varying from 1 to 6, and the surface roughness of the plate. Local and average Nusselt numbers were calculated using experimental data on airflow behaviour in different areas of jet impingement. Compared to a smooth flat plate, the grooved surface showed a significant increase in both local and average Nusselt numbers, with the local Nusselt number increased by 11% and averaged Nusselt number by 15.23%. Heat transfer across various regions, including stagnant, transition, and wall jet, was studied under a uniform heat flux over a flat plate. Experimental results show that maximum heat dissipation occurs in the transition region for semi-circular grooved surfaces, while for smooth flat plates, it occurs in the stagnation region. The maximum percentage deviation was recorded as 15.23% with Reynolds number of 12000.

Cite this article as: Rathod AM, Jadhav CK, Tarte RS, Gulhane NP, Taler J, Taler D, et al. Heat transfer enhancement by laterally impinging air jet on semi-circular grooved surface. J Ther Eng 2025;11(3):811–823.

INTRODUCTION

The technique known as air jet impingement involves directing high-velocity air jets toward a surface or object. This method finds wide application across various industrial and technological settings, such as electronic devices, high-density electrical equipment, and gas turbine cooling. Air jet impingement is favored for its ability to efficiently

dissipate large amounts of heat and its ease of adjusting the targeted position. Several factors, including the Reynolds number, clearance (z/d) of the nozzle outlet to the target plate, and the radial distance from the stagnant point, influence heat transfer rates in these scenarios. Many researchers have studied the impact of jets on flat surfaces over the past few decades. Choukran et al. [1] experimentally investigated the effect of surface roughness on heat

*Corresponding author.

*E-mail address: amrathod_p21@me.vjti.ac.in

This paper was recommended for publication in revised form by Editor-in-Chief Ahmet Selim Dalkılıç



transfer enhancement. In their study, the Reynolds number ranged from 6500 to 19000, and the clearance between the nozzle outlet and target plate varied from 0.05 to 15. The roughness was created using cubic particles with a uniform distribution of 1 mm over the surface. Their findings revealed that the overall Nusselt values on the rough plate increased by 8.9% to 28% compared to a smooth plate. Additionally, their results showed that surface roughness increased turbulence intensity within the flow. Gau and Lee [2] examined heat flow and impingement cooling along walls roughened with triangular ribs. Their results indicated a significant decrease in heat transfer when using two different ribbed walls with rib-to-pitch height ratios of two and four, combined with nozzles of varying sizes. Katti and Prabhu [3] analyzed the local heat transfer distribution along a smooth plate subjected to impinging jets in various regions. Flow patterns and heat transfer properties were observed using the infrared thermal method. Directing the impinging jet onto a smooth target surface, they identified three significant zones: stagnancy, transition, and wall jet. Sagot et al. [4] conducted an experimental study to determine how axisymmetric lathe-worked grooves affect heat transfer from an impinging jet to the wall under steady wall temperature conditions. They analyzed the effect of jet Reynolds number, centered on the orifice diameter, with grooves that were either square or grooved in cross-section. Their findings revealed that heat transfer enhancements could reach up to 81% compared to a smooth flat plate. Also, Katti et al. [5] observed the effect of low Reynolds numbers on the cooling rate of normally impinging jets. The results indicated a secondary rise at $z/d = 0.5$ and a Reynolds number of 12,000. They noted that the maximum cooling rate occurred at a low Reynolds number ($Re < 12,000$) and at $z/d = 0.5$. Caliskan and Baskaya [6] conducted an experimental investigation on various ribbed surfaces to enhance heat transfer through impingement jets. Five ribbed surfaces with distinct rib heights and shapes were selected, maintaining a rib height (e) to rib pitch (p) ratio of 6. The results showed an enhancement ranging from 4% to 26.6% in the average Nusselt number for the V-shaped ribs (V-SR) design compared to a smooth flat plate. Barik et al. [7] performed a numerical investigation within a three-dimensional computational domain to evaluate the effectiveness of various protrusion surfaces on a small rectangular channel. They aimed to enhance heat dissipation by impinging an air jet normally on the primary flow. Tests were conducted on rectangular, triangular, and trapezoidal protrusions. The results showed that triangular protrusions enhanced heat transfer more effectively than the other shapes. Attalla and Salem [8] examined the heat transfer distribution resulting from a diagonally impinging jet issued from a circular nozzle. The experiment was conducted with Reynolds numbers varying from 1500 to 30,000 and inclination angles ranging from 95° to 45° . The results showed that as the angle of inclination decreases, the cooling rate also

decreases, and the heat transfer distribution shifts towards the elevated side of the plate. Kannan and Sundararaj [9] conducted a computational simulation to explore the impact of grooved surfaces on heat transfer by jet impingement. The numerical simulation utilized the ANSYS FLUENT software package with the SST K- ω turbulence model. Their findings indicated that the grooved surfaces had a detrimental effect on jet impingement heat transfer. However, they also observed that grooves led to an overall enhancement in heat transfer. Adimurthy et al. [10] studied the impact of surface roughness and jet confinement on the distribution of local Nusselt numbers and constant pressure along the wall of a flat plate when subjected to impingement by a laminar slot air jet. According to their findings, the highest wall static pressure across all configurations indicates that maximum heat dissipation occurs near the stagnation point and diminishes significantly as the gap between the nozzle and the plate widens. Adimurthy and Katti [11] examined that, in all configurations, the highest wall static pressure occurs at the stagnation point and decreases as the clearance between the nozzle and the target plate increases. Each rough surface design exhibits a sub-atmospheric zone up to $z/d = 4$. The influence of confinement is more pronounced at $z/d = 0.5$ due to increased jet recirculation. On rough surfaces with extended confinement lengths, particularly at high Reynolds numbers, secondary peaks in wall static pressure—resulting from flow acceleration behind detached ribs—are frequently observed. As a result, the potential core length increases. Their findings offer valuable insights into the investigated setup pressure distribution and flow characteristics. Umair and Gulhane [12] numerically examined heat transfer enhancement on pin fin surfaces by varying turbulence intensity and the turbulence Prandtl number. Using the shear stress turbulence model, they accurately predicted the Nusselt number curve for the flow regime under consideration. Their observations revealed that the pin fin surface disrupted boundary layer formation within the flow at each interval, affecting the local heat transfer rate. Hodges et al. [13] conducted an experimental investigation into cooling different target surfaces using an array of multi-jet impingements. Air jets with Reynolds numbers ranging from 4,600 to 30,200 were directed onto various orientations of rough surfaces. A novel temperature measurement method assessed the cooling rate at different locations. Their findings indicated that only one orientation effectively prevents the spent air from escaping. Additionally, they observed that surface roughness enhances heat transfer by 10% to 30%. Shukla and Dewan [14] conducted a numerical study to evaluate the effectiveness of various RANS-based turbulence models for slit jet impingement over detached and flat ribbed surfaces. They also examined the effects of Reynolds number, the position of the first rib, and rib-to-plate clearance on heat transfer properties. According to their research, heat transfer was positively impacted by increasing the

Reynolds number, rib clearance, and placing the first rib in the streamwise direction. Umair et al. [15] conducted a numerical simulation to identify differences in cooling curves for various target surface thicknesses. They discovered a threshold geometric thickness of 0.05, beyond which the differences in cooling curves disappeared. The heat dissipation rate at the impinging point and wall region was highest at this critical thickness. It was concluded that this critical thickness depends on the thermophysical properties of the target plate material. In an experimental setup, Nabadavis and Mishra [16] conducted a quantitative analysis of heat transfer induced by jet impingement on a flat plate. The parameters studied included constant wall heat flux, Reynolds number, and computational domain size. The highest heat transfer characteristics were observed at $z/d = 25$ with $Re = 20000$. Their observations indicated that the heat transfer rate increases as the Reynolds number of the jet rises. Siddique et al. [17] investigated the development of power law correlations and conducted a numerical analysis of the Nusselt number distribution for an air jet from a straight circular nozzle impinging on a flat surface. Their study aimed to establish semi-empirical relationships that could predict the local Nusselt number based on various impinging jet and target surface properties. Their efforts led to the publication of semi-empirical power law relations, illustrating the magnitude of the local Nusselt number within the range of $Pr \times t/d < 0.012$. Jeyajyothi and Kalaichelvi [18] conducted a study to examine the increase in heat transfer and flow structure resulting from a jet impinging on a flat surface. They investigated how various performance factors affect the heat dissipation rate across the flat surface. Their findings revealed that maximum heat dissipation is achieved with a small clearance (z/d) between the nozzle outlet and the target plate, higher jet velocity, and a larger nozzle diameter. Additionally, they observed that the cooling rate decreases as the flow moves away from the impinging point. Mohd et al. [19] focused on establishing an empirical relationship to illustrate the variations in the Nusselt number profile and conducted a numerical investigation of non-dimensional constants. It is common practice to convert the temperature profile to the Nusselt profile when non-dimensionality poses challenges. However, as the Reynolds number exceeds 6,000, the profile becomes less irregular. Their results suggest that the development of turbulence vortices near the nozzle's exit is responsible for the reduction in variation in the Nusselt number profile. Secchi et al. [20] performed Direct Numerical Simulation (DNS) of a turbulent jet at $Re = 10,000$, both on smooth and rough surfaces. The mean radial velocity profiles, scaled by inner layer units, demonstrated that the roughness sublayer, influenced by the roughness topographies, extends into the outer layer of the wall jet. They concluded that surface roughness increases flow drag and inhibits the expansion of the radial-wall jet. Rathod et al. [21] conducted a numerical analysis to investigate the cooling rate of a flat surface

jet impingement with varying heat flux. Using a K-Omega SST turbulence model, they precisely projected the Nusselt curve in each flow zone. Semi-empirical correlations were developed for the stagnation, transition, and wall jet zones, aiding in the design of cooling systems for different heat flux conditions. Talapati and Katti [22] investigated the effects of curvature ratios on heat transfer efficiency. They found that higher curvature ratios ($D/d = 8.6$) focus heat transmission around the stagnation point, resulting in lower heat transfer coefficients. In contrast, lower ratios ($D/d = 4.28$) promote wider dispersion and improve average heat transfer. They also observed that, in a seven-jet configuration, decreasing the z/d and s/d values led to optimal heat transfer, reducing jet contact and increasing efficiency. The uniformity of heat transfer was measured using the coefficient of variance. In a related study, Talapati and Katti [23] examined the effects of various parameters on jet impingement local heat transfer properties. They investigated how the Reynolds number ($Re = 12,000$ to $28,000$), nozzle length to diameter ratio ($L/D = 0.5$ to 83), and clearance between nozzle outlet to plate ($z/D = 0.2$ to 2) influenced the heat transfer properties. They found that flow acceleration effects caused by vena-contracta shift the peak Nusselt number (Nu) from the stagnation point to the wall jet zone at lower z/D ratios. A variation of $\pm 16\%$ from the maximal heat transfer rate under ideal conditions in the stagnation area is revealed by the correlation. For a jet Reynolds number of 20000, Talapati and Katti [24] conducted an experimental study to explore the effects of varying the number of mounts beneath detachable ribs on heat transfer enhancement at different clearances of nozzle outlet to surface ($z/d = 0.5$ to 6). The results consistently show increased heat transfer in the stagnation zone compared to a smooth, flat surface. Due to the increased turbulence intensity from flow recirculation and vortex generation behind the mounts, detachable ribs with six mounts exhibit the greatest improvement in average Nusselt numbers (58%) at $z/d = 0.5$. Talapati et al. [25] also studied the impact of jet inclination angles ($45^\circ, 60^\circ,$ and 75°) and Reynolds numbers (12,000–28,000) on inclined circular air jet impingement on a flat plate. Using IR thermal imaging to investigate heat transfer characteristics, they found that the peak heat transfer position shifts uphill from the impingement point as the jet inclination decreases. At shorter clearance of nozzle outlet to the target plate and higher Reynolds numbers, the Nusselt number (Nu) values peaked further from the geometric center, resulting in a noticeable asymmetry in the Nu distribution across the plate. Additionally, Talapati et al. [26] compared parabolic, conical, and exponential nozzle designs over Reynolds numbers of 12,000–23,500 and jet to plate distances of 0.5–6 to investigate the effects of nozzle geometry on submerged turbulent jet flow characteristics over a smooth flat surface. They observed a secondary peak in the jet flow at $z/d = 6$ and approximately $r/d = 0.4$, indicating a laminar-to-turbulent transition on the plate. Parabolic nozzles

consistently produce higher heat transfer values due to their streamlined flow and reduced pressure losses, suggesting their potential for optimizing local heat transfer applications. In another study, Talapati and Katti [27] examined the impact of synthetic air jet temperature on local heat transmission as it impinges on a smooth flat surface. Significant increases in the Nusselt number were observed at $z/d = 1$ across frequencies ranging from 100 Hz to 300 Hz and jet-to-orifice lengths of 1 to 8 when using jet air temperature relative to ambient air temperature. They suggested that the synthetic air jets temperature significantly affects the distribution of heat transfer, especially when the orifice and jet were closer. Furthermore, Talapati et al. [28] investigated synthetic air jets local heat transfer properties of a over a convex surface. Their experimental investigation showed that the optimal conditions for improved heat transfer efficiency were found at $f = 200$ Hz and $z/d = 2$. There was an 18% variance in the correlation between the highest local Nusselt number and the Reynolds number, with less than $\pm 6\%$ uncertainty in the average Nusselt number observations.

The literature highlights the importance of heat transfer characteristics of semi-circular grooved surfaces, as most research has predominantly focused on ribbed, V-groove, and smooth flat surfaces. Rough surfaces have been identified as effective surface turbulators for enhancing heat transfer in both internal flows and jet impingement applications. However, research examining jet impingement on semi-circular grooved surfaces is sparse. These grooved surfaces have the potential to generate additional turbulence, which could further improve heat transfer. Therefore, the current objective is to explore the impact of semi-circular grooved surfaces on heat transfer enhancement during jet impingement. This study analyzes heat transfer by varying the clearance (z/d) between the nozzle outlet and the target plate surface for jet Reynolds numbers ranging from 4000 to 12000.

The current work aims to experimentally examine the augmentation of heat transfer in three distinct zones as defined by Katti and Prabhu [3]. These zones are: The stagnation zone ($0 < r/d < 1$) is located right below the impinging jet and is where the flow initially comes into contact with the surface. The jet's direct collision causes a substantial heat transfer rate. The transition zone ($1 < r/d < 2.5$) represents the flow transition from the high-velocity impact zone to a more developed flow. The flow starts to spread out and lose momentum, influencing heat transfer properties. The wall-jet zone ($r/d > 2.5$) is the farthest from the impinging point, where the flow spreads along the surface, forming a wall jet. This study examines the orthogonal impingement of an air jet on a semicircular groove while altering the clearance (z/d) of the nozzle outlet to the target plate and Reynolds number. Additionally, the heat transmission rates of the semicircular groove plate and the flat plate are compared to evaluate the overall performance enhancement provided by the grooved surface in each zone.

EXPERIMENTAL METHODOLOGY

Figure 1 shows a schematic configuration for the steady jet impingement setup. It includes a turbine blower, nozzle, electric heater, exhaust blower, control panel, and data acquisition system (DAQ). The air blower draws the ambient air into the flexible pipe connected to the plenum, which helps form of uniform velocity profile. The blower can circulate air at a rate of $200 \text{ m}^3/\text{hr}$, operating at a maximum speed of 2870 rpm. The airflow rate can be controlled using the frequency drive in the control panel to achieve the desired velocity at the nozzle inlet. The nozzle plate assembly, attached at the lower end of the plenum, secures nozzles of different diameters to vary air velocities for single or multiple jet types. The clearance between the nozzle outlet to the target plate can be adjusted using a mechanism provided with the nozzle assembly. A monometer measures the pressure at the plenum entrance with precision $\pm 0.3 \text{ N/m}^2$. The airflow rate at the nozzle exit is measured using hot-wire anemometer with an accuracy of $\pm 0.5 \text{ m/s}$. The nozzle is a steel pipe with a diameter of 15 mm. The target plate used in this study is aluminium plate with dimension of $100 \times 100 \text{ mm}$ and a thickness of 6 mm. The target plate is placed above the heater assembly using a C-clamp, as shown in Figure 2. Four k-type thermocouples, with an uncertainty of $\pm 0.5 \text{ }^\circ\text{C}$, are placed between the heater and the plate to ensure accurate temperature readings. The heater is initially started with uniform heat input (VI) of 3000 W/m^2 provided to the target surface to achieve steady state condition. The blower is turned on, and the air impinges on the target surface at given the flow rate. The surface temperature decreases over time and stabilizes at steady state condition, where temperature recordings are noted. Figure 2 shows the actual photograph of the experimental setup. Figure 3 provides a 2D schematic view of semi-circular grooved plate, offering detailed information about its structure. The plate has six circular grooves on the surface, each with a diameter of 6 mm and depth of 3 mm, placed uniformly at a distance of 11 mm, as shown in Figure 3.

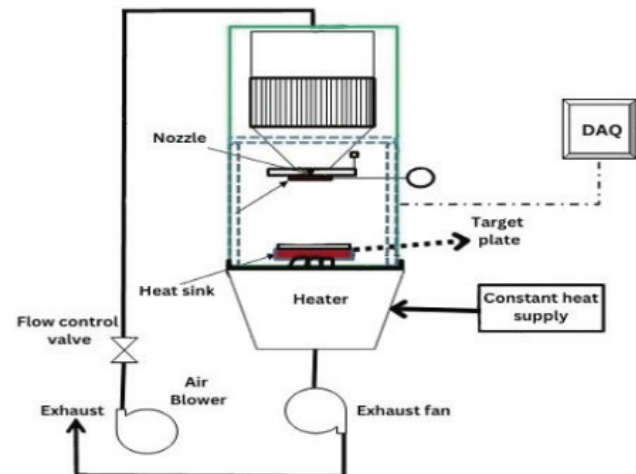


Figure 1. Schematic layout of an experimental setup.

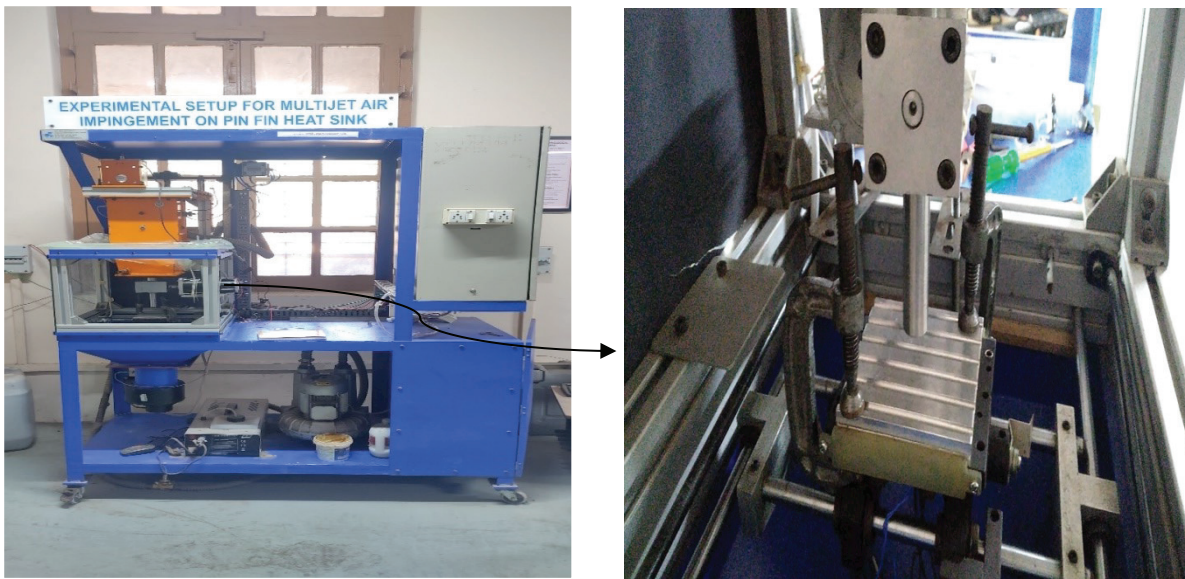


Figure 2. Semi Circular grooved plate assembly for heat transfer distribution.

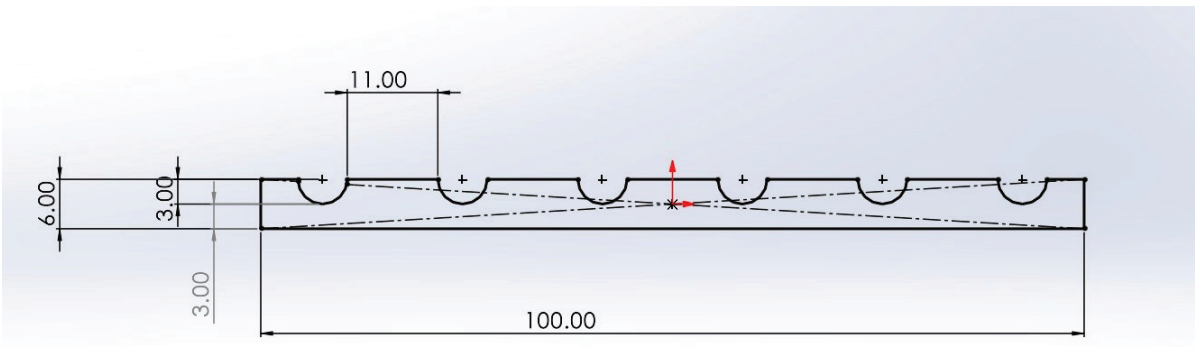


Figure 3. 2D layout of Semicircular grooved plate (all dimensions are in mm).

Data Reduction

The rate of convective heat transfer from a surface to a fluid medium can be determined using the equation (1).

$$h = \frac{q}{\Delta T} \quad (1)$$

The local Nusselt number is obtained using equation (2)

$$Nu = h \times \frac{d}{k} \quad (2)$$

The average Nusselt number can be written as

$$Nu_{avg} = \bar{h} \times d/k \quad (3)$$

Uncertainty Analysis

Evaluating uncertainty in an experimental study plays a crucial role in minimizing the potential errors in the

results. This study follows the method proposed by Everts and Meyer [29]. For a variable x_i with a known uncertainty δx_i , the variables and uncertainty are express in the following form:

$$x_i = x_i \text{ (measured)} \pm \delta x_i \quad (4)$$

The overall uncertainty in a result is usually denoted by equation (5), where R is the result of the experiment, ∂x_i is the uncertainty in one variable and δR is the overall uncertainty in the result.

$$\delta R = \left\{ \sum_{i=1}^n \left[\frac{\partial R}{\partial x_i} * \delta x_i \right]^2 \right\}^{1/2} \quad (5)$$

The uncertainty in the Nusselt number is calculated using the uncertainties of the following parameters: Nusselt number uncertainty, the uncertainties of the nozzle diameter (δD), specific heat capacity (δC_p), thermal conductivity

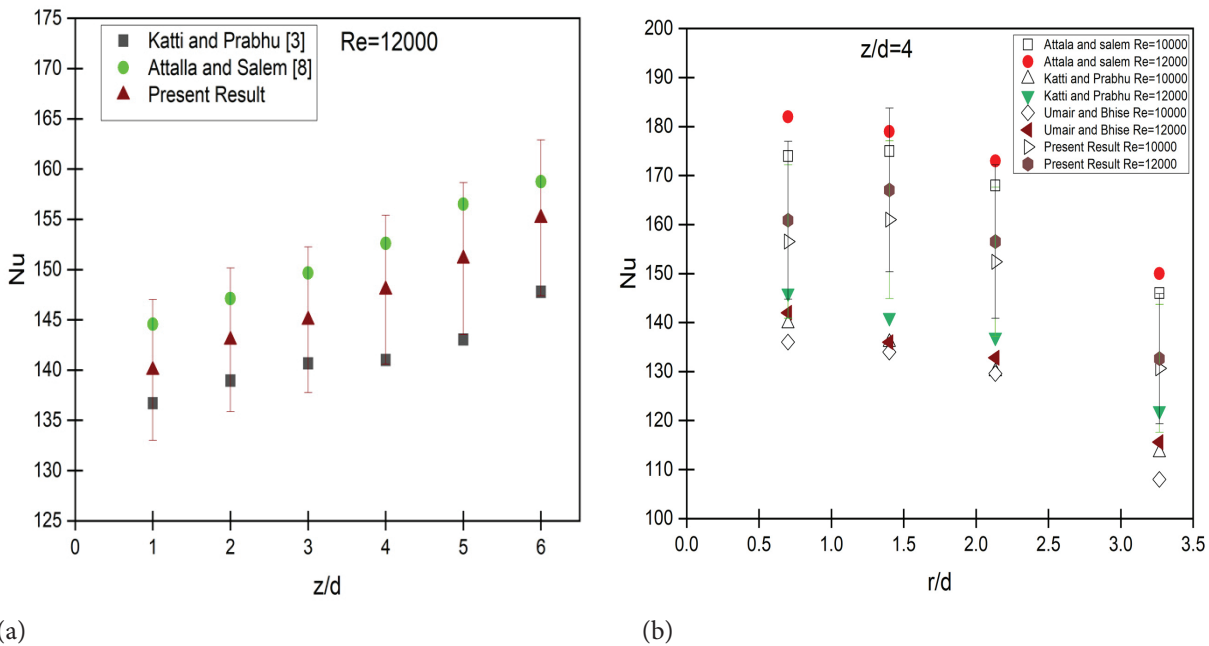


Figure 4. Comparison of local Nusselt number (a) with varying z/d (b) with varying Reynolds number.

(δk), bulk fluid temperature (δT_b), surface temperature (δT_s), surface area (δA), heat flux (δq) and heat transfer coefficient (δh).

$$\delta Nu = \left[\left(\frac{\partial Nu}{\partial h} \delta h \right)^2 + \left(\frac{\partial Nu}{\partial D} \delta D \right)^2 + \left(\frac{\partial Nu}{\partial k} \delta k \right)^2 \right]^{1/2} \quad (6)$$

$\delta Nu = 21.33$ (12.55%)

Hence, the uncertainty in the Nusselt number is found to be 12.55 %.

RESULTS AND DISCUSSION

Experiments were carried out on single circular infringement jet cooling of both smooth and rough (semi-circular grooved) surfaces. The studies were performed with a Reynolds number (Re) of 4000-12000 and a clearance (z/d) of the nozzle outlet to the target plate of 1 to 6. Variations in local and average Nusselt values across the radial direction were observed.

Validation of Present Results with Those Published in the Literature

Figures 4 (a) and 4 (b) compare the current experimental results with the empirical correlations provided by Katti and Prabhu [3], Attalla and Salem [8], and Siddique et al. [17]. Figure 4 (a) shows the local Nusselt number displayed at a constant Reynolds number of 12000 with z/d values ranging from 1 to 6. The maximal Nusselt magnitude was determined to be 155. Figure 4 (b) shows a comparable local Nusselt number profile displayed for Reynolds numbers 10000 and 12000, with a constant z/d of 4. The greatest

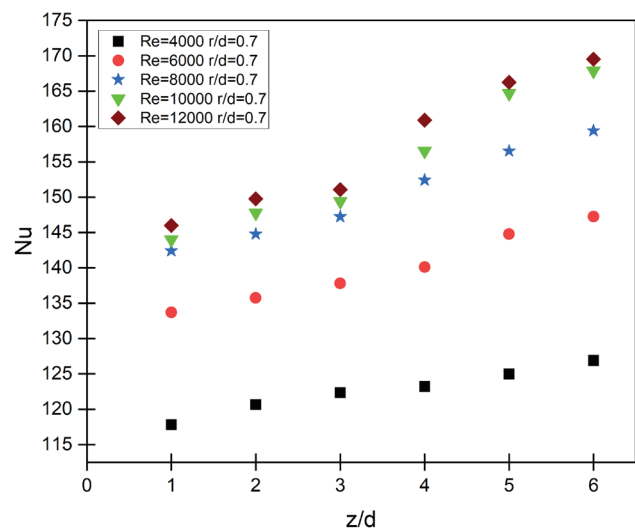


Figure 5. Local heat transfer distribution of semi-circular groove at stagnation region with varying Reynolds number.

local Nusselt number was discovered at Re = 12000 at the stagnation point of 168. The approximate percentage error between the current and provided literature results lies between 12% and 15%.

Deviation of Local Nusselt Number with Varying Reynolds Number in Stagnation Region

Experimental results were obtained for Reynolds numbers (Re) ranging from 4000 to 12000 at a stagnation point of r/d = 0.7. Figure 5 shows the graph between the Nusselt number and the clearance (z/d) of the nozzle outlet to

the target plate at $r/d = 0.7$. The results indicate that heat transfer increases with the Reynolds number. The maximum heat transfer was observed at $Re = 12000$, with a local Nusselt number of 168.2 at $z/d = 6$, and the minimum was observed at $z/d = 1$, with a local Nusselt number of 117.8. This enhancement is primarily due to increased fluid acceleration, which enhances turbulent intensity at lower r/d values. It was also observed that the Reynolds number is a strong determinant of heat transfer at the stagnation point. Also, the heat transfer coefficient was observed to decrease along radial direction up to the stagnation zone due to boundary layer formation.

Deviation of Local Nusselt Number with Varying Reynolds Number in Transition Region

The air flow from the stagnation zone to the wall jet zone undergoes a transition where the boundary layer shifts from laminar to turbulent. This transition continues in the radial direction from radial distance of $r/d = 1$ to approximately $r/d = 2.5$. Figure 6 illustrates the relationship between the local Nusselt number and the clearance (z/d) of the nozzle outlet to the target plate at transition regions $r/d = 1.4$ and $r/d = 2.133$. The figure shows that the Nusselt number increases with Reynolds numbers from 4000 to 12000 and decreases with increasing r/d along z/d . Additionally, the shear stress concentration across the wall in the radial direction was examined for different values of z/d ($1 < z/d < 6$). It was observed that shear stress sharply increases for all z/d values from r/d of 1 to 2.133. The maximum local Nusselt number was observed in the transition region at $z/d = 6$, with a local Nusselt number (Nu_{local}) of 176.4. It was also observed that heat transfer coefficient is higher in transition region compared to the stagnation region.

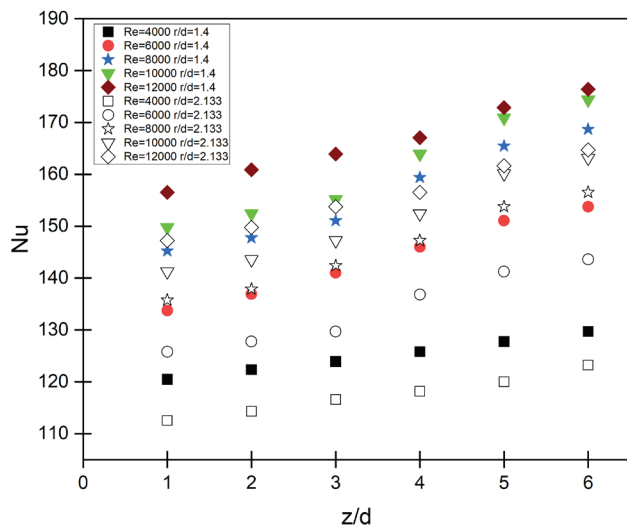


Figure 6. Local heat transfer distribution of semi-circular groove at transition region with varying Reynolds number.

Deviation of Local Nusselt Number with Varying Reynolds Number in Wall-Jet Region

Figure 7 represents the relationship between the Nusselt number and clearance (z/d) of the nozzle outlet to target plate at wall jet region of $r/d = 3.266$. It shows that the Nusselt number falls monotonically from the transition region to the wall jet region. At $r/d = 3.266$, the heat transfer rate was calculated, revealing that the Nusselt number increase with Reynolds number ranging from 4000 to 12000 along z/d . However, there was a decrement observed along radial distance (r/d). The observed decrease in the Nusselt number in the wall jet region can be attributed to the reduction in fluid velocity over flat plate caused radial flow. Additionally, the high interchange of momentum between the wall jet and

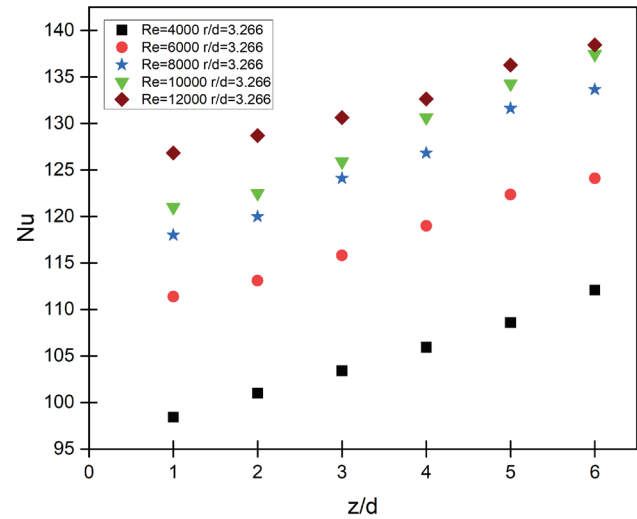


Figure 7. Local heat transfer distribution of semi-circular groove at wall-jet region with varying Reynolds number.

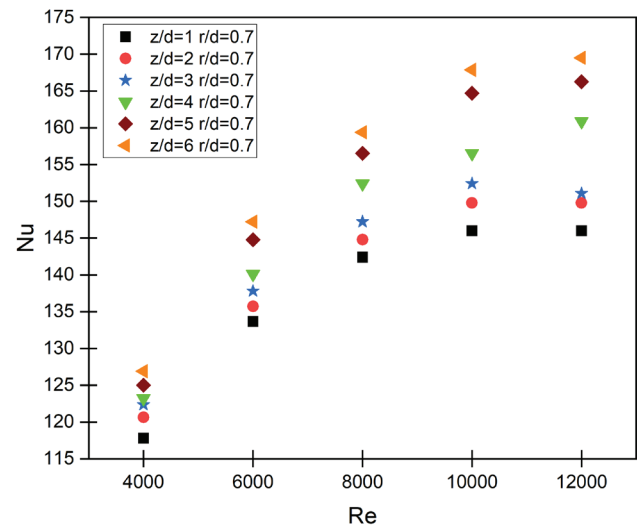


Figure 8. Local heat transfer distribution of semi-circular groove at stagnation region with varying z/d .

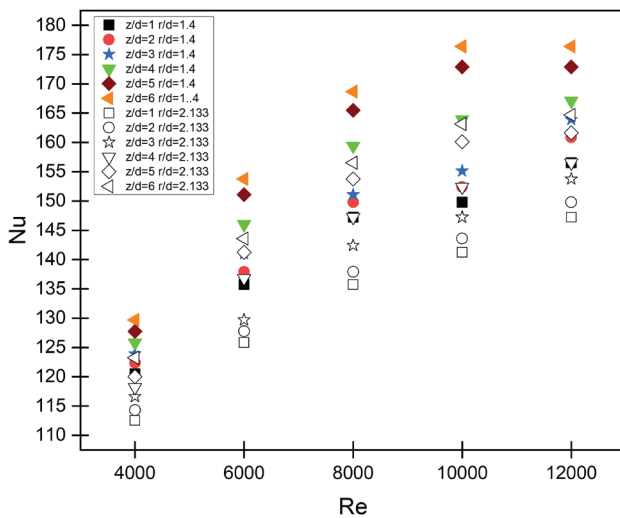


Figure 9. Local heat transfer distribution of semi-circular groove at transition region with varying z/d .

ambient air contribute to this decrease. This momentum exchange causes a loss of kinetic energy in the fluid, resulting in a lower heat transfer coefficient and a corresponding decrease in the Nusselt number.

Deviation of Local Nusselt Number with Varying Clearance of the Nozzle Outlet to Target Plate in Stagnation Region

The Figure 8 illustrates the relationship between the Nusselt number and Reynolds number, varying with the clearance (z/d) of the nozzle outlet to target plate. Notably, as both the clearance and Reynolds numbers increases, the Nusselt number also rises. This trend is particularly evident at stagnation point (r/d) of 0.7. The data suggests a positive correlation between Nusselt number and clearance (z/d) of the nozzle outlet to target plate and Reynolds number, indicating enhanced heat transfer with greater clearance and flow velocity. At stagnation region momentum of jet is maximum and it decreases as move away from the impinging point.

Deviation of Local Nusselt Number with Varying Clearance of the Nozzle Outlet to Target Plate in Transition Region

In Figure 9, Nusselt number magnitude are depicted for Reynolds numbers ranging from 4000 to 12000 at radial positions of $r/d = 1.4$ and 2.133 . The Nusselt number rises as the clearance (z/d) between the nozzle outlet and target plate extends from 1 to 6. The highest Nusselt number was observed at radial distance of $r/d = 1.4$, and it gradually decreases at radial distance of $r/d = 2.133$. The increase in the Nusselt number magnitude with greater clearance (z/d) is primarily due to the formation of a fully developed velocity profile and turbulent intensity generated by the grooved surface.

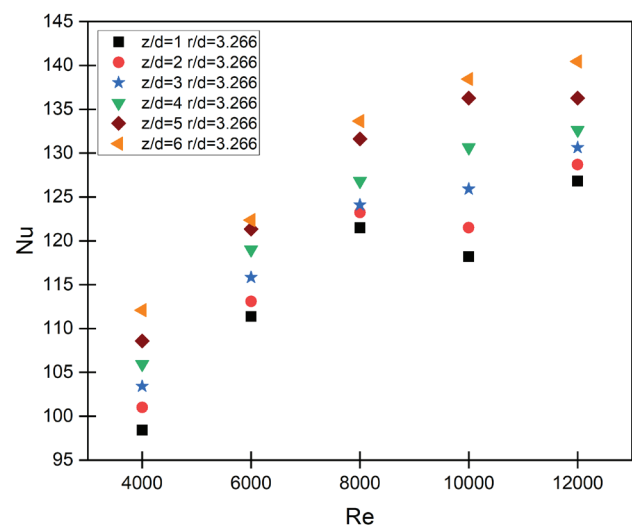


Figure 10. Local heat transfer distribution of semi-circular groove at wall-jet region with varying z/d .

Deviation of Local Nusselt Number with Varying Clearance of Nozzle Outlet to Target Plate in Wall-Jet Region

Figure 10 shows that the Nusselt number magnitude gradually decreases in the wall jet region for all clearances (z/d) between the nozzle outlet and target plate. This decrease in the Nusselt number is primarily due to reduction in fluid velocity over a flat plate as the flow moves radially outward. As the jet spreads, the velocity diminishes because of the increasing distance from the impinging point. In addition, there was momentum loss occurred between the wall jet and ambient air, which further reduces the velocity and consequently, the heat transfer rate.

Comparative Study of Local Nusselt Number on Semi-Circular Grooved Surface and Flat Surface Under Varying Reynolds Number

Figure 11 presents a comparison graph of local Nusselt numbers for both flat and groove surfaces across varying Reynolds numbers. The figure includes six graphs, all of which shows an increasing trend in Nusselt number as the Reynold number rises. The graph clearly shows that semi-circular groove surfaces have higher Nusselt values than smooth flat surface at the same Reynolds number and z/d ratio. The experimental readings highlight the significant impact of surface roughness on jet impingement. Specially, the heat transfer rate is higher in transition region of semi-circular grooved surface compared to the stagnation region of smooth surface. This is attributed due to higher turbulent mixing and fluid acceleration by grooved surface. The maximum local Nusselt number (Nu_{local}) for semicircular grooved surface is 176.4 at $z/d = 6$ and $Re=12000$, while for the smooth surface, the maximum local Nusselt number (Nu_{local}) is 155.2.

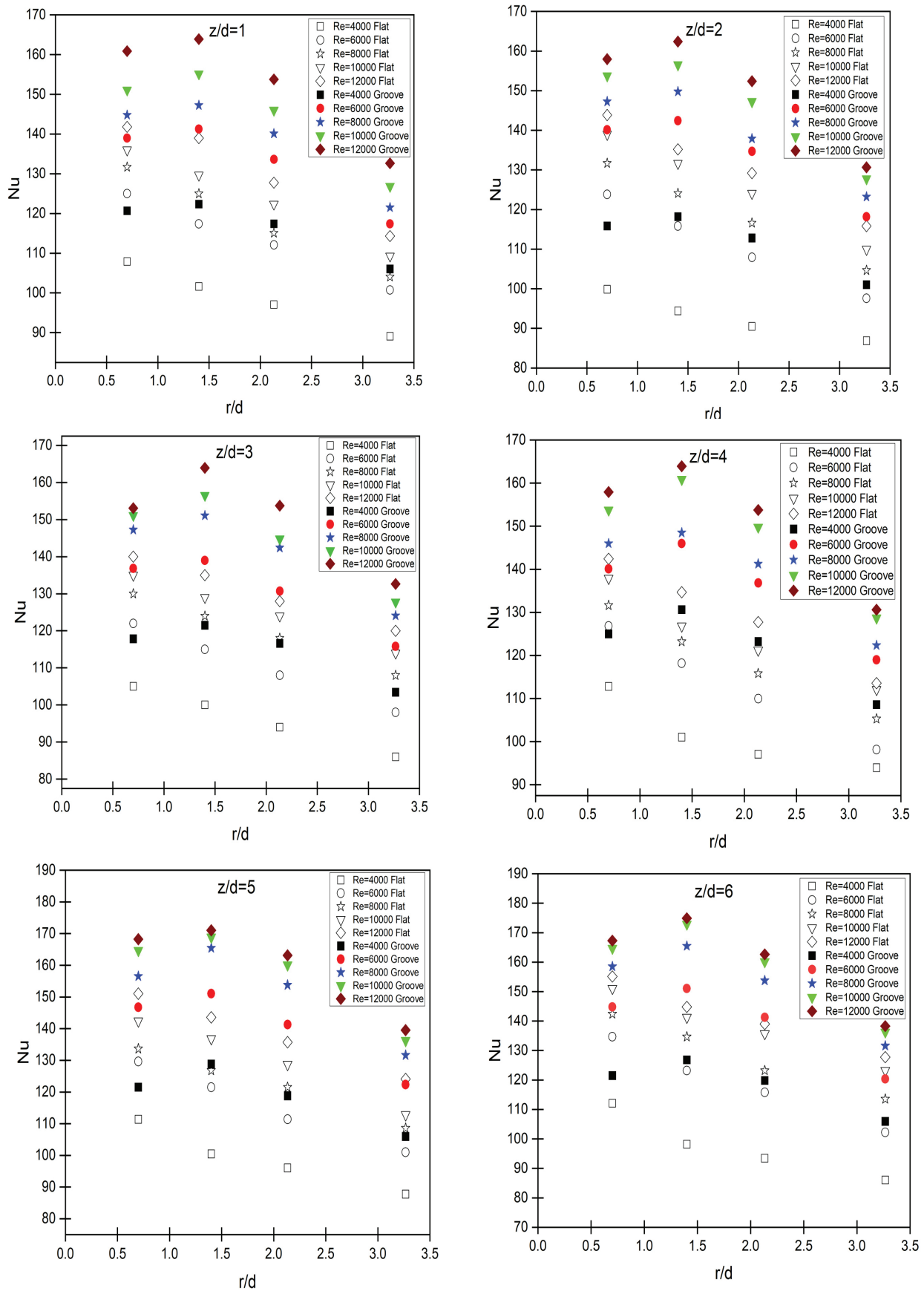


Figure 11. Local heat transfer distribution between semicircular groove and flat plate with varying Reynolds number.

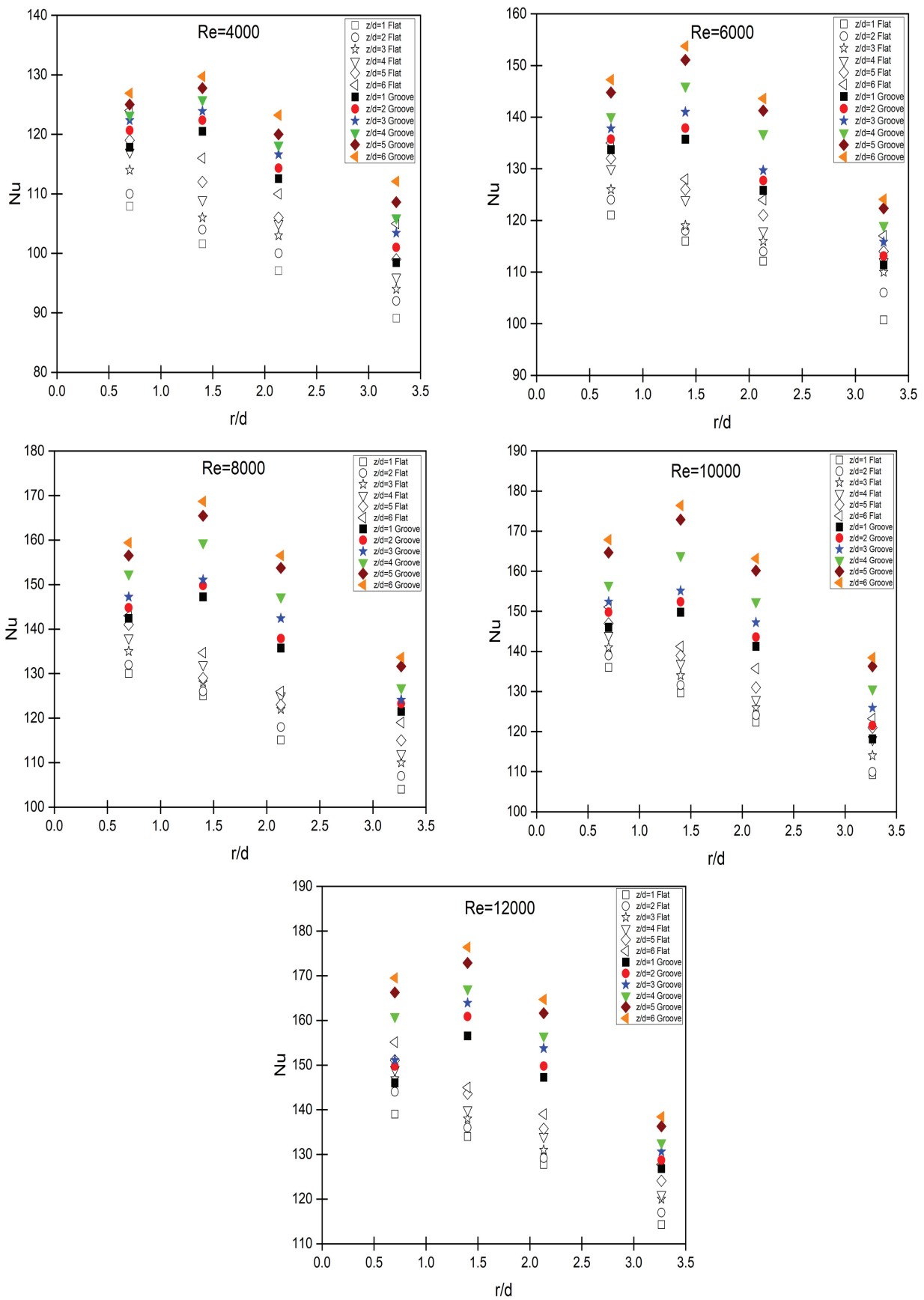


Figure 12. Local heat transfer distribution between semicircular groove and flat plate with varying Reynolds number.

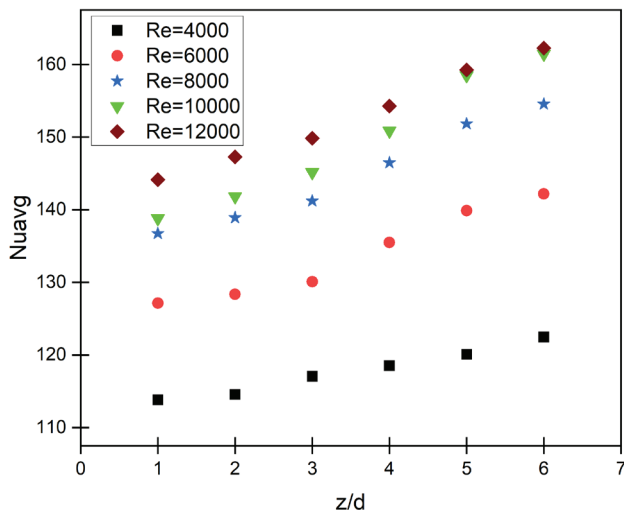


Figure 13. Average heat transfer distribution between semicircular groove plate by varying Reynolds number.

Comparative Study of Local Nusselt Number on Semicircular Grooved Surface and Flat Surface Under Varying Clearance of the Nozzle Outlet to Target Plate

Figure 12 presents a comparison graph of local Nusselt numbers for both smooth and groove surfaces across varying clearances (z/d) of the nozzle outlet to target plate. Figure include five graphs, all of which follow the same trend of increasing Nusselt numbers for increasing clearance (z/d) values. This trend occurs because of a larger clearance leads to a more uniform velocity and higher turbulence intensity with increasing clearance (z/d) values. The maximum local Nusselt number (Nu_{local}) for semicircular grooved surface is 176.4 at $z/d = 6$ and $Re=12000$, while for the smooth surface, the maximum local Nusselt number (Nu_{local}) is 155.2.

Effect of Clearance of the Nozzle Outlet to Target Plate on Average Nusselt Number at Various Reynolds Number

Figure 13 depicts the relationship between Reynolds number and clearance (z/d) in calculating the average Nusselt number for jet impingement on a grooved surface. Higher Reynolds numbers and appropriate clearances increase heat transfer rates, resulting in higher average Nusselt numbers. The grooved surface significantly amplifies these effects, emphasizing the importance of both flow dynamics and surface properties in heat transfer applications.

Table 1 presents a comparison of the average Nusselt numbers for flat and grooved plates at Reynold number of 12000, with clearance of the nozzle outlet to target plate varying from 1 to 6 ($1 < \frac{z}{d} < 6$). The table shows that the maximum percentage deviation, 15.23%, occurs at $z/d = 6$. This discrepancy is due to the flow becoming more developed at higher z/d ratios.

Table 1. Average Nusselt number deviation

z/d	Nu _{avg}		% Deviation
	Flat Plate	Groove Plate	
1	126.46	144.15	13.98
2	129.02	147.28	14.15
3	132.10	150.86	14.20
4	136.60	156.27	14.40
5	138.62	159.26	14.88
6	141.67	163.25	15.23

CONCLUSION

An experimental study was conducted to evaluate the localized variation of the heat transfer coefficient of a semicircular grooved plate and compare the results with a flat plate in three critical areas. The parameters varied, include the Reynolds number (ranging from 4000 to 12000) and the clearance of the nozzle outlet to the target plate (from 1 to 6). The following observations were made:

1. The study primarily focuses on three regions: the stagnation region ($z/d < 1$), the transition region ($1 < z/d < 2.5$), and the wall jet region ($r/d > 2.5$).
2. It was observed that as the Reynolds number increases, the cooling rate also increases along radial distances for all clearances (z/d).
3. For a constant Reynolds number, the Nusselt number increases in all regions with an increase in the clearance (z/d) of the nozzle outlet to the target plate. This may be due to increased near-wall turbulence intensities with greater clearance.
4. The highest heat transfer rate was observed in the stagnation region on the smooth flat plate at a given Reynolds number. Conversely, the highest heat transfer rate was observed in the transition region for the semicircular grooved plate. This may be due to the orientation of the grooves just away from the impingement point.
5. The maximum local Nusselt number and average Nusselt number were observed at $z/d = 6$ and $Re = 12000$, with values of 176.4 and 163.25, respectively. The maximum percentage deviation of 15.23% was noted when comparing the two plates at a Reynolds number of 12000.

NOMENCLATURE

Nu	Local Nusselt number
Nu_{avg}	Average Nusselt number
r	Radial distance of thermocouple from centre (m)
d	Diameter of nozzle (m)
z/d	Clearance of the nozzle outlet to target plate
q	Constant heat flux (W/m^2)
Re	Reynolds number

T_s	Temperature of thermocouple ($^{\circ}\text{C}$)
T_{∞}	Ambient temperature ($^{\circ}\text{C}$)
h	Heat transfer coefficient ($\text{W}/\text{m}^2\text{K}$)
k	Thermal conductivity of air (W/mK)
t/d	Geometric thickness of the target plate to nozzle diameter
Pr	Prandtl number
s/d	Jet to jet spacing
D/d	Lower curvature ratio
x/d	Axial distance from the stagnation point on convex surface to orifice diameter

AUTHORSHIP CONTRIBUTIONS

Authors equally contributed to this work.

DATA AVAILABILITY STATEMENT

The authors confirm that the data that supports the findings of this study are available within the article. Raw data that support the finding of this study are available from the corresponding author, upon reasonable request.

CONFLICT OF INTEREST

The authors declared that there are no known conflicts of interest regarding the research work of this research.

ETHICS

There are no ethical issues with the publication of this manuscript.

REFERENCES

- [1] Chakroun WM, Abdel-Rahman AA, Al-Fahed SF. Heat transfer augmentation for air jet impinged on a rough surface. *Appl Therm Eng* 1998;18:1225-1241. [\[CrossRef\]](#)
- [2] Gau C, Lee IC. Flow and impingement cooling heat transfer along triangular rib-roughened walls. *Int J Heat Mass Transf* 2000;43: 4405-4418. [\[CrossRef\]](#)
- [3] Katti V, Prabhu SV. Experimental study and theoretical analysis of local heat transfer distribution between smooth flat surface and impinging air jet from a circular straight pipe nozzle. *Int J Heat Mass Transf* 2008;51:4480-4495. [\[CrossRef\]](#)
- [4] Sagot B, Antonini G, Buron F. Enhancement of jet-to-wall heat transfer using axisymmetric grooved impinging plates. *Int J Therm Sci* 2010;49:1026-1030. [\[CrossRef\]](#)
- [5] Katti VV, Yasaswy SN, Prabhu SV. Local heat transfer distribution between smooth flat surface and impinging air jet from a circular nozzle at low Reynolds numbers. *Heat Mass Transf* 2011;47:237-244. [\[CrossRef\]](#)
- [6] Caliskan S, Baskaya S. Experimental investigation of impinging jet array heat transfer from a surface with V-shaped and convergent-divergent ribs. *Int J Therm Sci* 2012;59:234-246. [\[CrossRef\]](#)
- [7] Barik AK, Mukherjee A, Patro P. Heat transfer enhancement from a small rectangular channel with different surface protrusions by a turbulent cross flow jet. *Int J Therm Sci* 2015;98:32-41. [\[CrossRef\]](#)
- [8] Attalla M, Salem M. Experimental investigation of heat transfer for a jet impinging obliquely on a flat surface. *Exp Heat Transf* 2015;28:378-391. [\[CrossRef\]](#)
- [9] Kannan BT, Sundararaj S. Steady state jet impingement heat transfer from axisymmetric plates with and without grooves. *Proc Eng* 2015;127:25-32. [\[CrossRef\]](#)
- [10] Adimurthy M, Katti VV, Venkatesha. Experimental study of fluid flow and heat transfer characteristics of rough surface, impinged by a confined laminar slot air jet. *IJERT* 2016;5:1-6. [\[CrossRef\]](#)
- [11] Adimurthy M, Katti VV. Experimental investigations on the local distribution of wall static pressure coefficient due to an impinging slot air jet on a confined rough surface. *Int J Eng Technol Manage Appl Sci* 2016;4:69-78.
- [12] Umair SM, Gulhane NP. On numerical investigation of heat transfer augmentation through pin fin heat sink by laterally impinging air jet. *Proc Eng* 2016;157:89-97. [\[CrossRef\]](#)
- [13] Hodges J, Osorio A, Fernandez EJ, Kapat JS, Gangopadhyay T, Sen S, et al. An experimental investigation of an array of inline impinging jets on a surface with varying rib orientations and blockages. *Proceedings of the ASME Turbo Expo, American Society of Mechanical Engineers (ASME)*, June 26-30, 2017, Charlotte, North Carolina, USA. [\[CrossRef\]](#)
- [14] Shukla AK, Dewan A. Convective heat transfer enhancement using slot jet impingement on a detached rib surface. *J Appl Fluid Mech* 2017;10:1615-1627. [\[CrossRef\]](#)
- [15] Umair SM, Kolawale AR, Bhise GA, Gulhane NP. On numerical heat transfer characteristic study of flat surface subjected to variation in geometric thickness. *Int J Comp Mater Sci Eng* 2017;6:1750010. [\[CrossRef\]](#)
- [16] Nabadavis A, Mishra DP. Jet impingement heat transfer on a plate with axisymmetric square grooves—a numerical investigation. *Int J Eng Technol Sci Res* 2018;5:1-6.
- [17] Siddique UM, Bhise GA, Gulhane NP. On numerical investigation of local Nusselt distribution between flat surface and impinging air jet from straight circular nozzle and power law correlations generation. *Heat Transf Asian Res* 2018;47:126-149. [\[CrossRef\]](#)
- [18] Jeyajothi K, Kalaihelvi P. Augmentation of heat transfer and investigation of fluid flow characteristics of an impinging air jet on to a flat plate. *Arab J Sci Eng* 2019;44:5289-5299. [\[CrossRef\]](#)

- [19] Mohd US, Ansari E, Khan SA, Gulhane NP, Patil R. Numerical investigation of nondimensional constant and empirical relation representing Nusselt profile nonuniformity. *J Thermophys Heat Transf* 2020;34:215–229. [\[CrossRef\]](#)
- [20] Secchi F, Gatti D, Frohnapfel B. The wall-jet region of a turbulent jet impinging on smooth and rough plates. *Flow Turbulence Combust* 2023;110:275–299. [\[CrossRef\]](#)
- [21] Rathod AM, Gulhane NP, Siddique UM. Heat transfer augmentation for impingement of steady air jet under exponential heat flux boundary condition. *Int J Eng* 2023;37:920–930. [\[CrossRef\]](#)
- [22] Talapati RJ, Katti VV. Local heat transfer characteristics of circular multiple air jet impinging on a semicircular concave surface. *Exp Heat Transf* 2023;37:851–874. [\[CrossRef\]](#)
- [23] Talapati RJ, Katti VV. Influence of ratio of nozzle length to diameter on local heat transfer study of an unconfined circular air jet impingement. *Int J Therm Sci* 2023;183:107859. [\[CrossRef\]](#)
- [24] Talapati RJ, Katti VV. Influence of turbulator under the detached rib on heat transfer study of air jet impinging on a flat surface. *Int J Therm Sci* 2023;184:107946. [\[CrossRef\]](#)
- [25] Talapati RJ, Baghel K, Shrigondekar H, Katti VV. Influence of inclined unconfined circular air jet impingement on local heat transfer characteristics of smooth flat plate. *Int J Therm Sci* 2024;197:108848. [\[CrossRef\]](#)
- [26] Talapati RJ, Hiremath NS, Katti VV. Influence of nozzle geometry on wall static pressure coefficient of the submerged turbulent jet impinging on a smooth flat surface. *Int J Ambient Energy* 2023;44:1959–1968. [\[CrossRef\]](#)
- [27] Talapati RJ, Katti VV. Influence of synthetic air jet temperature on local heat transfer characteristics of synthetic air jet impingement. *Int Comm Heat Mass Transf* 2022;130:105796. [\[CrossRef\]](#)
- [28] Talapati RJ, Katti VV, Hiremath NS. Local heat transfer characteristics of synthetic air jet impinging on a smooth convex surface. *Int J Therm Sci* 2021;170:107143. [\[CrossRef\]](#)
- [29] Everts M, Meyer JP. Test sections for heat transfer and pressure drop measurements: construction, calibration, and validation. In: Meyer J, De Paepe M, eds. *The Art of Measuring in the Thermal Sciences*. Boca Raton: CRC Press; 2020. p. 53. [\[CrossRef\]](#)